

- und H. Stegemeyer, Ber. Bunsenges. Phys. Chem. 78, 883 (1974).
- [11] H. de Vries, Acta Crystallogr. 4, 219 (1951).
- [12] S. Chandrasekhar und K. N. Srinivasa Rao, Acta Crystallogr. A 24, 445 (1968).
- [13] H. Kelker, Mol. Cryst. Liq. Cryst. 15, 347 (1972).
- [14] G. Heppke und F. Oestreicher, Z. Naturforsch. 32a, 899 (1977).
- [15] H. J. Krabbe, H. Heggemeier, B. Schrader und E. H. Korte, J. Chem. Res. (S) 1978, 228; (M) 1978, 3023.
- [16] E. Gil-Au, B. Feibush und R. Charles-Sigler, Tetrahedron Lett. 10, 1009 (1966).
- [17] E. Langer und H. Lehner, Monatsh. Chem. 110, 1003 (1979).

(Eingegangen am 10. September 1979) E 4431

## The Electrooxidation of Glucose in Phosphate Buffer Solutions : Kinetics and Reaction Mechanism \*)

S. Ernst, J. Heitbaum

Institut für Physikalische Chemie, Wegelerstraße 12, D-5300 Bonn

C. H. Hamann

Angewandte Physikalische Chemie, Universität Oldenburg, POB 2503, D-2900 Oldenburg

*Elektrochemie / Adsorption / Biophysikalische Chemie / Massenspektroskopie*

The electrochemical oxidation of glucose on Pt at pH = 7.5 within  $400 \leq \varphi_{\text{RHE}} \leq 800$  mV was studied by cyclic voltammetry, by taking quasistationary current-potential curves, by measuring the surface coverage of organic residues, and by analyzing the primary reaction product. The results can be summarized as follows:

1. Glucono lactone is the only reaction product being formed by the anodic process. Gluconic acid is generated by hydrolysis.
2. Tafel lines had to be normalized for the uncovered surface with the help of the adsorption measurements. The apparent transfer coefficient is  $\alpha_{\text{app}} = 0.37 \pm 0.03$ .
3. The electrochemical reaction orders of glucose and  $\text{H}^+$  were determined to be  $z_{\text{G}} = 0.35 \pm 0.04$  and  $z_{\text{H}^+} = -0.38 \pm 0.04$ , resp.

These results are interpreted by means of a reaction mechanism. The kinetic parameters measured are confirmed by a model calculation.

Die anodische Oxidation der Glucose an Pt bei pH = 7,5 im Potentialbereich  $400 \leq \varphi_{\text{RHE}} \leq 800$  mV wurde mit Hilfe der zyklischen Voltammetrie, durch Aufnahme quasistationärer Strom-Potentialkurven, durch Messung des Bedeckungsgrades mit organischer Substanz sowie durch Analyse des Primärproduktes der Reaktion untersucht. Die Ergebnisse können wie folgt zusammengefaßt werden:

1. Als einziges Reaktionsprodukt entsteht Gluconsäurelacton im elektrochemischen Prozeß. Gluconsäure wird durch eine nachgelagerte Hydrolyse gebildet.
2. Tafel-Geraden mußten mit Hilfe der Adsorptionsmessungen auf die adsorbatfreie Oberfläche normiert werden. Als scheinbarer Durchtrittsfaktor wurde  $\alpha_{\text{app}} = 0,37 \pm 0,03$  gefunden.
3. Die elektrochemischen Reaktionsordnungen von Glucose und  $\text{H}^+$  sind  $z_{\text{G}} = 0,35 \pm 0,04$  bzw.  $z_{\text{H}^+} = -0,38 \pm 0,04$ .

Diese Ergebnisse werden auf der Grundlage eines Reaktionsmechanismus gedeutet. Die gemessenen kinetischen Parameter werden anhand einer Modellrechnung bestätigt.

### 1. Introduction

The use of implantable glucose/oxygen fuel cells as power sources for artificial hearts or cardiac pace-makers would have the advantage that both the fuel and the oxygen can be taken from the blood the reaction products being eliminated by the natural metabolism [1]. The same holds for a glucose sensor developed in relation to an artificial pancreas [2, 3]. The life time of such a glucose/oxygen fuel cell would only be determined by the stability of the catalysts used as electrodes. Experiments in vitro and in vivo have been already performed [2].

With respect to the medical applications mentioned the electrooxidation of glucose on platinum was investigated by several authors [4–6] mainly by cyclic voltammetry. The adsorption behavior was studied by galvanostatic loading

curves [1, 4]. The conclusions drawn differ insofar as Yao et al. [5] believe the cyclic form of the glucose molecule to be reactive while Giner et al. [1] as well as Skou [6] propose the selective oxidation of the aldehyde. A model of the kinetics of the process was lacking up to now.

Therefore the elementary steps of the anodic oxidation of glucose on Pt at pH = 7.5 were examined. Special efforts were made to identify the intermediates and products this being significant not only for the reaction mechanism but with respect to the corporal compatibility in the case of the medical applications mentioned.

### 2. The Physico-Chemical and Electrochemical Characteristics of Glucose

Glucose exists in two optical isomer hemiacetalic ring forms ( $\alpha, \beta$ -glucose) differing in the position at the anomeric  $\text{C}_1$ -atom. The mutual conversion in aqueous solution is acid-

\*) Partly presented on the 76. Hauptversammlung der Deutschen Bunsen-Gesellschaft, Braunschweig 1977.

base catalyzed and proceeds via a ring opening to the aldehyde ( $\gamma$ -glucose) [7] as is shown in Fig. 1.

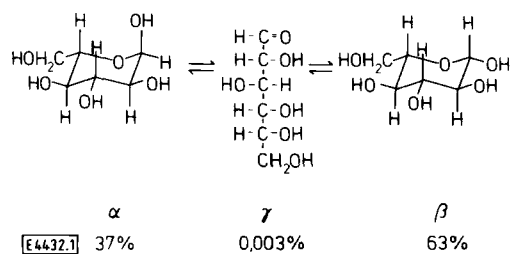


Fig. 1

Stable forms of glucose in an aqueous solution, relative concentrations after [7]

The hemiacetalic OH-group is a stronger acid ( $pK_s \approx 12.3$ ) [8] than the alcoholic ( $pK_s \approx 16$ ) [9] so that the hydrogen atom being bond to the C<sub>1</sub>-atom is somewhat activated and any oxidation process should first attack at this point. Indeed, gluconic acid was found to be the oxidation product both in homogeneous [10, 11] chemical and electrochemical [12] reactions.

According to Fig. 2, the anodic oxidation can either start with  $\alpha, \beta$ -glucose, in which case the glucono lactone should be formed as the first intermediate, or the aldehyde can be oxidized to gluconic acid directly. The glucono lactone undergoes hydrolysis with a rate constant of  $10^{-3} \text{ s}^{-1}$  at  $\text{pH} = 7.5$  and  $20^\circ\text{C}$  [13] which corresponds to a half life of about 10 min. In any case, gluconic acid should be the stable product of a two electron oxidation.

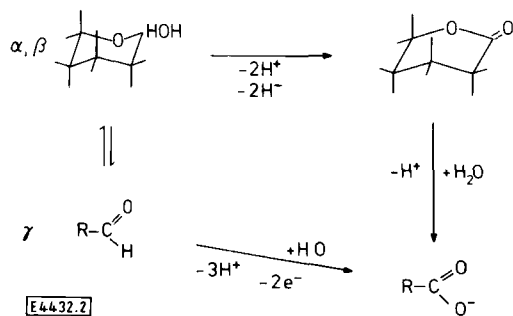


Fig. 2

Principle reaction paths for the two electron oxidation of glucose

Qualitatively, for the electrochemical oxidation of glucose on Pt three potential regions can be distinguished as can be seen from Fig. 3:

1. At  $150 \leq \phi_{\text{RHE}} \leq 350 \text{ mV}$  relatively high current peaks are observed which are related to an exceptional reactivity of glucose being discussed in a previous paper [14].
2. The glucose oxidation within the so called double layer region ( $400 \leq \phi_{\text{RHE}} \leq 800 \text{ mV}$ ) is relevant for the fuel cell applications mentioned above and will be considered below.
3. At potentials more positive than 1100 mV a reaction of glucose with the Pt-O layer occurs which was not investigated in detail.

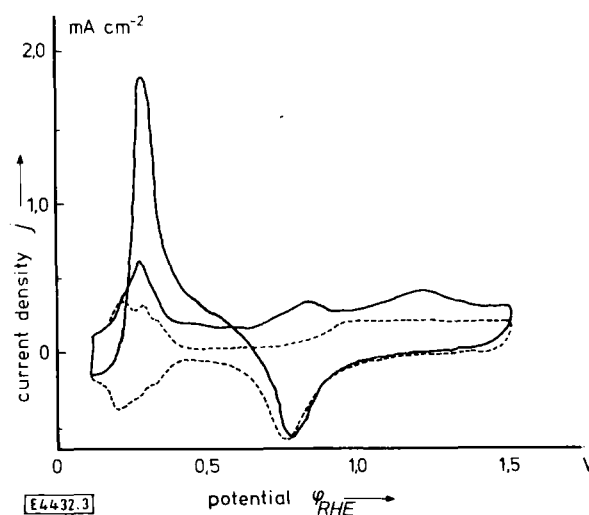


Fig. 3

Current-potential diagram of 0.1 M glucose on Pt in phosphate buffer  $\text{pH} = 7.5$ ,  $I = 1.5 \text{ M}$ ,  $v = 100 \text{ mV s}^{-1}$ ,  $T = 295 \text{ K}$ ; dotted: surface layer diagram of base electrolyte

### 3. Experimental

*Qualitative results* were obtained by cyclic voltammetry the method being well established in the Ref. [15]. Reaction orders and the apparent transfer coefficient were measured by recording quasistationary current-potential curves at a sweep rate of  $5 \text{ mV s}^{-1}$ .

The *adsorption of organic residues* (glucose and/or products) was studied by measuring the pseudocapacity of hydrogen. This method is described in the previous paper [14].

The *analysis of a reaction product* requires its sufficiently high concentration. On Pt, however, the glucose oxidation is a self inhibiting process at all oxidation potentials. Furthermore, the glucono lactone, if it is formed as an intermediate, decomposes as was mentioned above. Consequently, the *time of electrolysis must not exceed 100 s*. In order to achieve a product concentration of about  $10^{-3} \text{ mol l}^{-1}$  within this time, a microelectrolysis cell was constructed which is shown schematically in Fig. 4. It has a very small volume of anolyte ( $0.01 \text{ cm}^3$ ) being in contact with the platinized working electrode (roughness factor 150). The compartment of the counter and reference electrode is separated by a dialysis membrane and can easily be removed in order to withdraw a sample with a microliter syringe. Separated conduits allow the anolyte volume to be filled with base electrolyte or glucose solution, resp., both being deaerated previously. Thus, the electrode could be activated at first and then brought into contact with the glucose solution under potential control. Electrolysis was performed under potentiostatic conditions. The charge ( $10^{-7} \text{ F}$  at maximum) was measured with a current integrator.

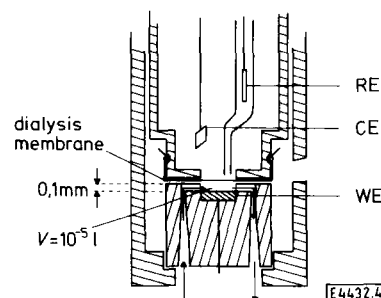


Fig. 4

Microelectrolysis cell

The analysis was accomplished with a mass spectroscopic method developed by Röllgen and coworkers [16] using a small droplet of the electrolyte which was transferred to a 10  $\mu\text{m}$  tungsten wire. Organic molecules are ionized by alkali ion attachment under the influence of a high electric field and detected in a quadrupole mass filter.

An indirect proof for the formation of the lactone would be the detection of the delayed protons being formed by hydrolysis (cf. Fig. 2). Therefore pH-time curves were recorded after electrolysis bringing a droplet of the solution onto the plane membrane of a special pH-electrode (Ingold, type LOT 403-M8).  $\text{CO}_2$  uptake from air was prevented by putting the pH-electrode in a closed glass flask partly filled with the buffer solution. 0.1 M diphosphate buffer was used within these experiments because its titration curve shows a relatively high and uniform pH-change in the neutral region.

All chemicals used were of the highest purity available (p. A. or biochemical grade) and were solved in Millipore water. The phosphate buffers between pH = 5.5 and 8.0 were adjusted to a constant ionic strength of  $I = 1.5 \text{ mol l}^{-1}$  by adding  $\text{K}_2\text{SO}_4$ .

Working and counter electrode were prepared from 99.999% smooth platinum, for electrolysis the working electrode was platinized. As the reference electrode either a  $\text{Hg}/\text{HgSO}_4$ - or a hydrogen electrode in the base electrolyte was used. The latter consisted of a glass tube closed at the top and containing a platinized Pt-net its upper part being surrounded by a pure hydrogen atmosphere previously produced by cathodic hydrogen evolution [17]. All potentials reported are related to the hydrogen potential in the same solution.

The electrolyte was deaerated by bubbling Argon before and in between the experiments.

## 4. Results

### 4.1. Cyclic Voltammetry

The current-potential diagram of Fig. 5 shows that the glucose oxidation within the double layer region starts at a potential as low as 400 mV. This means, that the reaction hardly can be catalyzed by a Pt-OH layer, but glucose is directly oxidized. At 670 and 750 mV two neighboring current peaks can be distinguished which overlap at higher sweep rates ( $v > 5 \text{ mV s}^{-1}$ ). The peak potentials are shifted towards more positive values when the sweep rate is increased. Unfortunately, a more concrete analysis of the  $E_p$  vs.  $\log v$  and  $j_p$  vs.  $v^{1/2}$  relationships was not possible because of the two overlapping peaks.

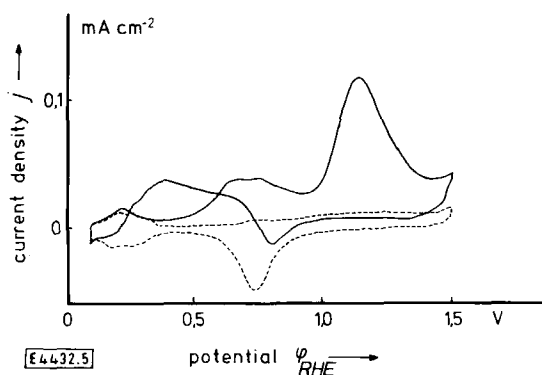


Fig. 5

Current-potential diagram of 0.1 M glucose on Pt in phosphate buffer pH = 7.5,  $I = 1.5 \text{ M}$ ,  $v = 5 \text{ mV s}^{-1}$ ,  $T = 295 \text{ K}$ ; dotted: surface layer diagram of base electrolyte

If the ionic strength  $I$  is increased, the peak current density  $j_p$  decreases as can be seen from Fig. 6. Evidently, the anion adsorption competes with the glucose oxidation as it was already stated by Skou [13]. In any case the peak current density is about two orders of magnitude smaller than it should be expected for a diffusion controlled process.

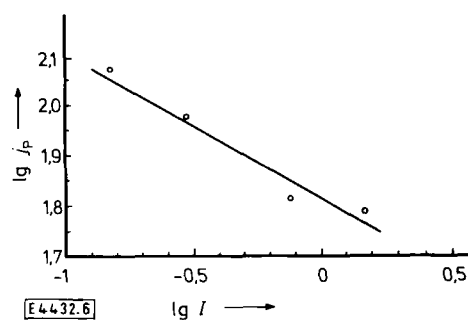


Fig. 6

Peak current density  $j_p$  of 0.1 M glucose on Pt as a function of ionic strength  $I$  of phosphate buffer pH = 7.5,  $v = 5 \text{ mV s}^{-1}$ ,  $T = 295 \text{ K}$  ( $j_p$  in  $\mu\text{A cm}^{-2}$ ;  $I$  in  $\text{mol l}^{-1}$ )

Furthermore, in a stirred solution, the current peaks in the double layer region become smaller. This unusual behavior was explained by Skou [13] assuming a heterogeneously formed endiol to be the electroactive species which is removed from the electrode under forced convection. Two observations are in contradiction to this assumption:

1. Sorbitol and Na-gluconate which are unable to form an endiol show the same behavior.
2. At a rotating electrode the current decreases with time the faster the angular frequency  $\omega$  is. But it is independent of the rotating speed when extrapolated to  $t = 0$ . This behavior should be expected when an inhibitor is transported from the solution to the electrode. In the case of the heterogeneously formed endiol no time dependence of the current should be observed but it should be strongly dependent on the angular frequency.

### 4.2. Adsorption

Fig. 7 shows the surface coverage of organic residues at Pt in two phosphate buffer solutions with different glucose concentration. The surface coverage was measured exactly under the same conditions at which the quasistationary current potential curves were recorded, i. e. the potential was kept constant at 200 mV for 5 min and then an anodic sweep with  $5 \text{ mV s}^{-1}$  was applied. When the potential desired was reached it was stepped to 20 mV and two cyclic voltammograms were recorded between 20 and 120 mV

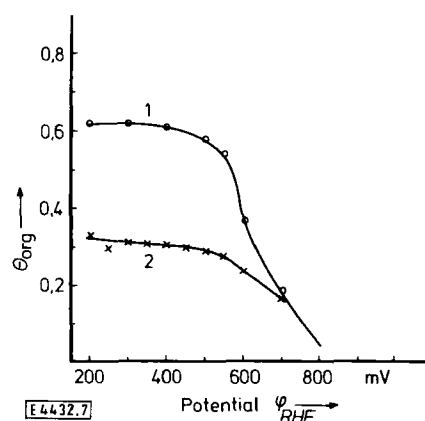


Fig. 7

Surface coverage  $\theta_{\text{org}}$  versus potential after waiting 300 s at  $\phi_{\text{RHE}} = 200 \text{ mV}$  and consecutive potential sweep with  $v = 5 \text{ mV s}^{-1}$ , phosphate buffer pH = 7.5,  $I = 1.5 \text{ M}$ ,  $T = 295 \text{ K}$ , 0.1 M (1) and 0.001 M (2) glucose

with a sweep rate of  $10 \text{ V s}^{-1}$ . From these the pseudocapacity of hydrogen was calculated and by comparison to the free surface the amount of adsorbed organic molecules was obtained [cf. 14].

As can be seen from Fig. 7, the surface coverage  $\theta_{\text{org}}$  is nearly constant up to 500 mV and then desorption starts. Moreover,  $\theta_{\text{org}}$  is independent of pH ( $5.5 \leq \text{pH} \leq 9$ ) but strongly dependent of the glucose concentration.

#### 4.3. Quasistationary Current-Potential Curves

When quasistationary current-potential curves were recorded, the difficulty arose that at the starting potential lying anywhere in the hydrogen region ( $\varphi_{\text{RHE}} < 350$  mV) glucose is oxidized. There-

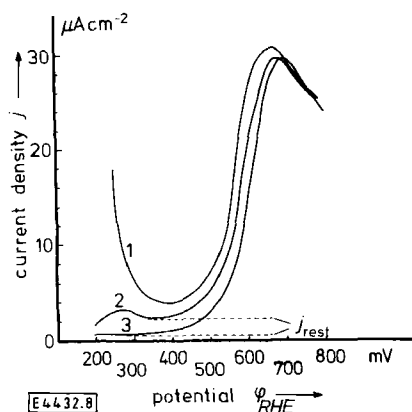


Fig. 8

Current-potential curves of 0.1 M glucose on Pt in phosphate buffer pH = 7.5,  $I = 1.5$  M,  $v = 5$  mV s<sup>-1</sup>,  $T = 295$  K, waiting times  $t_w = 0$  s (1), 60 s (2), and 300 s (3)

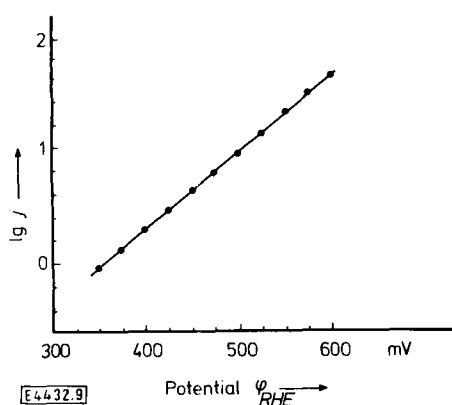


Fig. 9

Tafel-line of curve 3 in Fig. 8 normalized to  $\theta_{\text{org}} = 0$  ( $j$  in  $\mu\text{A cm}^{-2}$ )

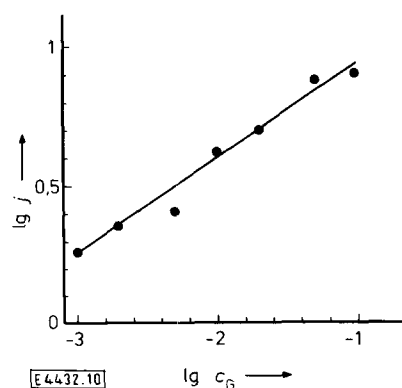


Fig. 10

Reaction rate at  $\varphi_{\text{RHE}} = 500$  mV normalized to  $\theta_{\text{org}} = 0$  as a function of glucose concentration, conditions as in Fig. 8 ( $j$  in  $\mu\text{A cm}^{-2}$ ;  $c_G$  in mol l<sup>-1</sup>)

fore the equilibrium concentration of glucose at the electrode is disturbed before the reaction under consideration takes place. But since the reaction in the hydrogen region declines rapidly, the potential was kept constant at  $\varphi_{\text{RHE}} = 200$  mV for a definite waiting time and only then the current-potential curve was measured. In Fig. 8 the effect of the waiting time is demonstrated. With  $t_w = 300$  s the reaction in the hydrogen region came almost to an end. The waiting time influences only slightly the peak potential and the peak current but does not affect the Tafel slope at all.

By waiting for 5 min at the starting potential an undisturbed concentration profile could be established, but by then the electrode is covered with an organic adsorbate which diminishes the reactive surface area. Therefore all curves had to be normalized to  $\theta_{\text{org}} = 0$  with the aid of the results described in the previous section. For this the following equation was used

$$i_{\text{corr}} = i_{\text{measured}}(1 - \theta_{\text{org}}). \quad (1)$$

Fig. 9 shows an example of a Tafel line taken with  $t_w = 300$  s and corrected to  $\theta_{\text{org}} = 0$ . In Fig. 10 the dependence of the reaction rate on the glucose concentration is given. Tafel slope, reaction orders with respect to glucose and protons and the apparent transfer coefficient are summarized in Table 1.

Table 1

Kinetic parameters of the glucose oxidation at Pt between 400 and 700 mV in phosphate buffer solution (pH = 7.5): values corrected to  $\theta_{\text{org}} = 0$

$z_G$	$z_{\text{H}^+}$	$b$ [mV]	$\alpha_{\text{app}}$
$0.35 \pm 0.04$	$-0.38 \pm 0.04$	$160 \pm 10$	$0.37 \pm 0.03$

#### 4.4. Analysis

Since phosphate buffer solutions proved to be unfavourable for the FD-mass-spectroscopic analysis, solutions of 0.1 M glucose in a NaHCO<sub>3</sub>-buffer at pH = 7.4 were used. Measurements were performed after electrolysis at different potentials between 300 and 400 mV. About  $10^{-7}$  moles of glucose were oxidized. Fig. 11 summarizes the results the peaks corresponding to [glucose + Na]<sup>+</sup> ( $m/e = 203$ ), [lactone + Na]<sup>+</sup> ( $m/e = 201$ ) and [gluconate + 2Na]<sup>+</sup> ( $m/e = 241$ ). Spectrum a exhibiting only the big glucose peak was taken from a fresh solution. Spectrum b was obtained 3 min after electrolysis and shows besides the glucose peak both lactone and gluconate. Finally, in spectrum c being recorded 30 min after electrolysis all the lactone being eventually formed has already decomposed to gluconate. These results indicate that the reaction proceeds at least partly via the formation of glucono lactone.

This was confirmed by the pH-measurements after electrolysis at various potentials between 150 and 1050 mV. Two examples

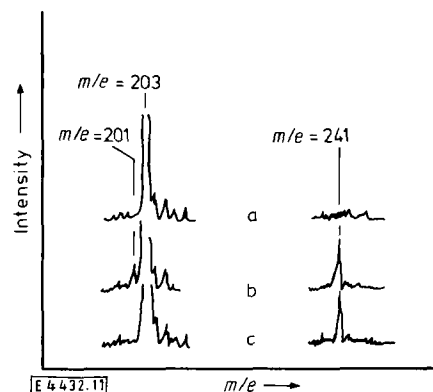


Fig. 11

Field-desorption mass spectra of 0.1 M glucose in sodium bicarbonate pH = 7.4 before electrolysis (a), 3 min after electrolysis (b), 30 min after electrolysis (c)

are given in Figs. 12 and 13. In all cases the pH decreases with time after the electrolysis thus indicating the formation of a delayed proton by the hydrolysis of the lactone. This result can be supported quantitatively. Considering  $n_s$  the number of protons spontaneously formed by electrolysis and  $n_d$  the number of protons generated by delayed hydrolysis and taking into account the actual titration curve,  $n_s/n_d$  amounts to  $2.0 \pm 0.13$ . Hence the lactone must be the only direct oxidation product within the accuracy of the experiment.

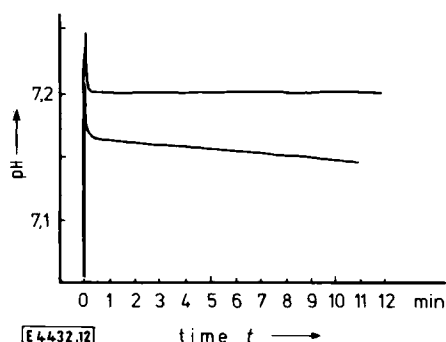


Fig. 12

pH-time curve of 0.1 M glucose in 0.1 M diphosphate buffer pH = 7.2 before electrolysis (upper curve) and after electrolysis at  $\varphi_{\text{RHE}} = 200$  mV;  $3 \cdot 10^{-8}$  moles of glucose were oxidized

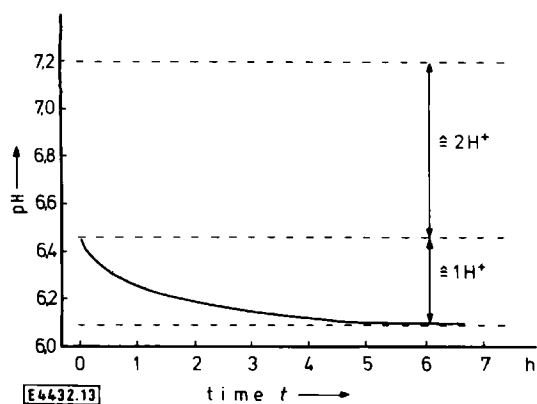


Fig. 13

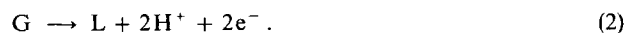
pH-time curve after electrolysis at  $\varphi_{\text{RHE}} = 1050$  mV, solution as in Fig. 12;  $3 \cdot 10^{-7}$  moles of glucose were oxidized

This shows the ring forms of glucose to be electroactive at Pt. The direct oxidation of the aldehyde to gluconic acid can only play the role of a side reaction corresponding to its low concentration (see above).

### 5. Discussion

The anodic oxidation of glucose between 350 and 800 mV was studied on an electrode surface partly covered with an adsorbate formed at 200 mV within the waiting time  $t_w$ . This adsorbate probably is a chemisorbed form of the lactone as was postulated previously [14]. Consequently, the reaction under consideration takes place on the remaining free surface covered by water molecules and anions which have to be displaced by glucose.

Since the lactone was found to be the only direct reaction product at all potentials, the electrochemical overall process can be symbolized as



What is to be explained are the values of the kinetic parameters given in Table 1. This will be done by the following arguments (1) and (2) and by the calculation given below.

1. The non integer reaction orders indicate adsorption processes to be involved in the mechanism. Since  $z_{\text{H}^+} = -z_{\text{G}} < 0$ , a preceding equilibrium reaction includes one glucose molecule and one proton as educt and product, resp. Furthermore, the splitting off of the second hydrogen atom must be rate determining, because otherwise  $z_{\text{H}^+} = -2z_{\text{G}}$  would have been measured.
2. The preceding dehydrogenation step could be either a homogeneous dissociation of the hemiacetalic OH-group or the heterogeneous splitting of the  $\text{C}_1-\text{H}$ -bond. Using the concept of the reaction layer [18] the kinetic current corresponding to a preceding homogeneous dissociation can easily be estimated by the equation

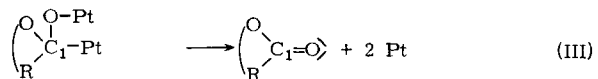
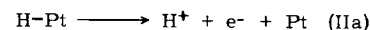
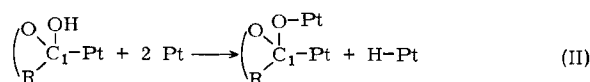
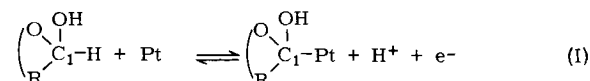
$$j_{\text{K}} = nF K_{\text{D}} c_{\text{G}} D_{\text{G}}^{1/2} (k_{\text{r}}/c_{\text{H}^+})^{1/2} \quad (3)$$

$K_{\text{D}}$  and  $k_{\text{r}}$  being the equilibrium constant and recombination constant of the dissociation reaction. By inserting the respective numerical values  $k_{\text{r}} \approx 10^{11} \text{ mol}^{-1} \text{ s}^{-1}$  [19],  $D_{\text{G}} \approx 5 \cdot 10^{-6} \text{ cm}^2 \text{ s}^{-1}$  [7],  $K_{\text{D}} \approx 3 \cdot 10^{-13} \text{ mol l}^{-1}$  [8],  $c_{\text{G}} = 10^{-3} \text{ mol l}^{-1}$  and  $c_{\text{H}^+} = 3 \cdot 10^{-8} \text{ mol l}^{-1}$  (at pH = 7.5) one obtains

$$j_{\text{K}} \approx 240 \mu\text{A cm}^{-2} \quad (4)$$

Since the peak current density under these conditions amounts only to  $j_{\text{p}} \approx 8 \mu\text{A cm}^{-2}$ , the homogeneous dissociation can be excluded.

Taking into account these arguments the mechanism can be visualized as follows



Assuming reaction (II) to be rate determining, the surface coverage  $\theta_1$  of the first intermediate  $\left( \begin{array}{c} \text{OH} \\ | \\ \text{O} \\ | \\ \text{R}-\text{C}_1-\text{Pt} \end{array} \right)$  can be assumed to be considerably greater than that of the lactone  $\theta_2$ . If reaction (I) is in equilibrium  $\theta_1$  is given by the electrochemical isotherm [20]

$$\frac{\theta_1}{1 - \theta_1} \exp(f_1 \theta_1) = K c_{\text{G}} c_{\text{H}^+}^{-1} \exp \frac{F\varphi}{RT} \quad (5)$$

$f$  being the heterogeneity factor, i.e. a measure of the change of the adsorption energy with coverage.

Assuming reaction (II) to be slow, the rate of the oxidation is given by

$$v_2 = k_2 \theta_1 \exp \{ -\gamma_{21} f_1 \theta_1 + (1 - \gamma_{22}) f_2 \theta_1 \} \quad (6)$$

Here the exponential term takes into consideration that the first intermediate desorbes under simultaneous dehydrogenation and that the lactone being formed is reabsorbed.  $\gamma_{21}$  and  $\gamma_{22}$  are the corresponding symmetry factors [20].

From Eq. (6) the reaction order of glucose can be calculated to give

$$z_G = \frac{\partial \ln v_2}{\partial \ln c_G} = \frac{\partial \ln \theta_1}{\partial \ln c_G} [1 - \theta_1(\gamma_{21}f_1 - (1 - \gamma_{22})f_2)]. \quad (7)$$

From Eq. (5) it follows that

$$\frac{\partial \ln \theta_1}{\partial \ln c_G} = \frac{1 - \theta_1}{1 + f_1\theta_1(1 - \theta_1)}. \quad (8)$$

By inserting Eq. (8) into Eq. (7) one obtains

$$z_G = \frac{1 - \theta_1 [1 - \theta_1(\gamma_{21}f_1 - (1 - \gamma_{22})f_2)]}{1 + \theta_1 f_1(1 - \theta_1)}. \quad (9)$$

The analogous calculation gives for the reaction order of the  $H^+$ -ions

$$z_{H^+} = - \frac{(1 - \theta_1) [1 - \theta_1(\gamma_{21}f_1 - (1 - \gamma_{22})f_2)]}{1 + \theta_1 f_1(1 - \theta_1)}. \quad (10)$$

Finally, the apparent transfer coefficient  $\alpha_{app}$  is determined by

$$\alpha_{app} = \frac{RT}{F} \frac{\partial \ln v_2}{\partial \varphi} = \frac{RT}{F} \frac{\partial \ln \theta_1}{\partial \varphi} [1 - \theta_1(\gamma_{21}f_1 - (1 - \gamma_{22})f_2)]. \quad (11)$$

Again, from Eq. (5) one obtains

$$\frac{\partial \ln \theta_1}{\partial \varphi} = \frac{F}{RT} \frac{(1 - \theta_1)}{1 + f_1\theta_1(1 - \theta_1)}. \quad (12)$$

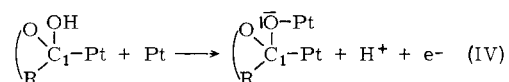
Consequently, the final result for  $\alpha_{app}$  is

$$\alpha_{app} = \frac{1 - \theta_1 [1 - \theta_1(\gamma_{21}f_1 - (1 - \gamma_{22})f_2)]}{1 + f_1\theta_1(1 - \theta_1)}. \quad (13)$$

Summarizing, the result of these calculations in accord with the kinetic parameters measured is

$$z_G = -z_{H^+} = \alpha_{app}. \quad (14)$$

Finally it should be mentioned, that alternatively to reaction (II) the following step could be rate determining.



This process is nothing but the sum of reactions (II) and (II a). In that case, the mathematical analysis proceeds exactly like

that given above with the exception that in Eq. (6) a potential dependent exponential function has to be added containing the transfer coefficient  $\alpha_2$  for the hydrogen ionisation step. The result would be an apparent transfer coefficient of

$$\alpha_{app} = z_G + \alpha_2$$

which is in contradiction to  $\alpha_{app} = z_G$  measured assuming  $\alpha_2 \approx 0.5$ . Therefore, it is to be concluded that only the mechanism given by the Eqs. (I)–(III) is in accord with the experimental results obtained.

We highly appreciate the help of Dr. H. J. Heinen who carried out the mass spectroscopic analysis. Financial support of this work by the DFG is gratefully acknowledged.

### References

- [1] J. Giner and P. Malachuky, Proc. Artif. Heart Program. Conf., US. Dept. Health, Education and Welfare 1969, p. 839.
- [2] J. Giner, G. Hollek, and P. A. Malachuky, Ber. Bunsenges. Phys. Chem. 77, 782 (1973).
- [3] L. Marincić, J. S. Soeldner, C. K. Colton, J. Giner, and S. Morris, J. Electrochem. Soc. 126, 43 (1979).
- [4] M. L. B. Rao and R. F. Drake, J. Electrochem. Soc. 116, 334 (1969).
- [5] S. J. Yao, A. J. Appleby, and S. K. Wolfson, Jr., Z. Phys. Chem. NF 82, 225 (1972).
- [6] E. M. Skou, Electrochim. Acta 22, 313 (1977).
- [7] A. W. Fonds and J. M. Los, J. Electroanal. Chem. 36, 479 (1972).
- [8] J. J. Christensen, J. H. Rytting, and R. M. Izatt, J. Chem. Soc. (B), 1646 (1970).
- [9] P. Ballinger and F. A. Long, J. Am. Chem. Soc. 82, 795 (1960).
- [10] H. S. Isbell, H. L. Frush, C. W. R. Wade, and C. E. Hunter, Carbohydr. Res. 9, 163 (1969).
- [11] K. Heyns and O. Stöckel, Liebigs Ann. Chem. 558, 192 (1947).
- [12] K. Heyns and R. Heinemann, Liebigs Ann. Chem. 558, 187 (1947).
- [13] E. M. Skou, Thesis, Lyngby (Danmark) 1974.
- [14] S. Ernst, J. Heitbaum, and C. H. Hamann, J. Electroanal. Chem. 100, 173 (1979).
- [15] See for instance: J. Heitbaum and W. Vielstich, Angew. Chem. 86, 758 (1974).
- [16] F. W. Röhlgen, H. J. Heinen, and U. Giessmann, Naturwissenschaften 64, 222 (1977).
- [17] F. G. Will, private communication.
- [18] P. Delahay, New Instrumental Methods in Electrochemistry, p. 91–95, Interscience Publ., New York 1966.
- [19] A. Weller, Disc. Faraday Soc. 27, 28 (1959).
- [20] B. E. Conway, Determination of Mechanisms of Electrode Reactions Involving Adsorbed Species, in MTP Rev. of Sci., Phys. Chem. Ser. 1, Vol. VI, p. 80, Butterworths, London 1973.

(Eingegangen am 10. September 1979, E 4432  
endgültige Fassung am 18. Oktober 1979)